Hexamethylene-1,3-bis(cetyldimethylammonium bromide) protected low-toxicity ZnSe quantum dots as fluorescent probe for proteins

Yaping Zhong[1], *Chun Deng*[1], *Yu He*[1,2], *Yili Ge*[1,2], *Gongwu Song*[1,2]

[1]*Ministry-of-Education Key Laboratory for the Synthesis and Application of Organic Functional Molecules, College of Chemistry and Chemical Engineering, Hubei University, Wuhan 430062, People's Republic of China*
[2]*Hubei Collaborative Innovation Center for Advanced Organic Chemical Materials, College of Chemistry and Chemical Engineering, Hubei University, Wuhan 430062, People's Republic of China*
E-mail: heyu@hubu.edu.cn

Published in Micro & Nano Letters; Received on 25th November 2014; Revised on 29th December 2014; Accepted on 9th February 2015

Hexamethylene-1,3-bis(cetyldimethylammonium bromide) ($G_{16\text{-}6\text{-}16}$) protected low-toxicity ZnSe quantum dots (QDs) were successfully synthesised and used as fluorescence probe to detect proteins such as bovine serum albumin (BSA). This method is simple, fast, selective and sensitive. Surfactant $G_{16\text{-}6\text{-}16}$ can interact with proteins through hydrophobic effect, thus leading to the fluorescence quenching of $G_{16\text{-}6\text{-}16}$ protected ZnSe QDs nanometre material. The fluorescence intensity of $G_{16\text{-}6\text{-}16}$ protected ZnSe QDs was linearly proportional to BSA over a concentration range from 0 to 80 nM with a correlation coefficient of 0.993. The detection limit was 0.04 nM. This method was successfully applied to determine BSA in urine samples which shows the good application value of this nanometre material.

1. Introduction: Proteins play an important role in various biological processes [1]. Human serum and plasma proteomes are estimated to be composed of more than 10 000 different proteins in a dynamic range of protein concentration, most of which would be present at very low relative abundances [2, 3]. Interestingly, proteomics is entering into the field of biomedicine with declared hopes for the identification of new pathological markers and therapeutic targets [4]. Hence, the development of sensitive, selective and flexible methods for detecting proteins is highly demanded and of great significance.

Many methods, such as resonance light scattering techniques [5–7], chemiluminescence [8], Bradford assay method [9], circular dichroism, fluorescence spectroscopy [10], Fourier transform infrared spectroscopy [11] and differential scanning calorimetry [12], have been proposed for the detection of proteins. Expensive instruments or complicated sample preparation processes are required, although these methods are sensitive. Thus, efforts have been devoted to designing suitable and environmentally friendly sensors for protein detection. Unlike the above techniques, fluorescence methods offer a promising approach for simple, low-cost and rapid tracking of proteins.

Semiconductor nanocrystals, known as 'quantum dots' (QDs), have high luminescence efficiency, continuous excitation spectrum, high stability against photobleaching, controllable and narrow emission bands compared with the traditional organic fluorescent dyes, due to the quantum confinement effects [13–16]. Thus, they are ideal fluorescent dyes to replace organic fluorescent dyes and have attracted increasing interest for bioimaging [17], biolabelling [18], biodetection [19] and clinical diagnosis [20]. Compared with the traditional CdSe QDs that have toxicity in certain conditions [21], ZnSe QDs (without heavy metal ions) are potential blue fluorescent biological labels because of their low cytotoxicity [22–25]. ZnSe QDs as wide bandgap nanomaterials are excellent UV-blue emitters [26] complementary to those visible and near-infrared emitting QDs. Gemini surfactants are a relatively widely used new type of surfactant. They have a lower critical micelle concentration (CMCC) and a higher ability to reduce the oil/water interfacial tension and are comparable to conventional surfactants [27–30].

QDs possess negative charges because of the –COO– groups on the surface of the QDs, so they can combine with positively charged surfactants. In this study, we used the Gemini surfactant hexamethylene-1,3-bis(cetyldimethylammonium bromide) ($G_{16\text{-}6\text{-}16}$) to modify ZnSe QDs and have successfully synthesised $G_{16\text{-}6\text{-}16}$ protected low-toxicity ZnSe QDs. The interactions between the Gemini surfactant and proteins aroused researchers' attention more and more [31]. Serum albumin (ALB) is the most abundant protein in blood plasma, which plays an important role in maintaining plasma osmotic pressure, transporting a wide variety of compounds and balancing nutrition. Low levels of ALB may indicate liver and kidney troubles or malnourishment caused by a low-protein diet [32]. It is necessary to measure the ALB content in blood plasma or other biological fluids to obtain useful information about a patient's health. Bovine serum albumin (BSA) is frequently studied as a model protein because of its structural homology with human serum albumin [33]. Therefore, the development of analytical methods for BSA detection in biological samples has attracted much attention [34–36]. Chodankar *et al.* [37] proposed the mechanism of interaction between BSA and Gemini surfactant. As a high fluorescence efficiency nanomaterial that possesses excellent physical and chemical properties, $G_{16\text{-}6\text{-}16}$ protected ZnSe QDs have been introduced as a new fluorescent platform for sensing BSA. This method is simple, fast, selective and sensitive. Surfactant $G_{16\text{-}6\text{-}16}$ can interact with proteins through hydrophobic effect, thus leading to the fluorescence quenching of $G_{16\text{-}6\text{-}16}$ protected ZnSe QDs nanometre material [38] which facilitated our sensing approach. Furthermore, we validated the practicality of this method through an analysis of BSA in urine samples.

2. Experimental: Gemini surfactant $G_{16\text{-}6\text{-}16}$, BSA, Se, $CdCl_2{\cdot}2.5H_2O$ and MAP (3-mercaptopropionic acid) were purchased from Hubei University, Wuhan Tianyuan Biotechnology Co. Ltd., Tianjin Kermel Chemical Reagent Co. Ltd., Tianjin Suzhuang Chemical Reagent factory and Aladdin Reagent Co., Ltd., China, respectively. BSA was dissolved in methanol and a stock solution of 40 nM was prepared from which BSA was diluted to serial concentrations. All solutions were freshly prepared before use, and Milli-Q water (18 MΩ cm) was used throughout the experiments.

The crystalline structure and composition of the $G_{16\text{-}6\text{-}16}$ protected ZnSe QDs were identified by a D/MAX-IIIC X-ray

doi: 10.1049/mnl.2014.0698

diffractometer (Shimadzu, Japan). The morphology of the QDs was characterised by high-resolution transmission electron microscopy (HRTEM) on a Philips Tecnai G2 F20 (Philips, Holland) microscope operating at a 200 kV accelerating voltage. The UV–vis absorption measurements were performed on ZF-I three-operating UV analyser (Gucun Electricity Light Instrumental Factory, China). Fluorescence spectra were recorded on an RF-540 fluorophotometer (Tokyo, Japan) equipped with a 1.0 cm quartz cell and a thermostat bath.

Synthesis of ZnSe QDs: typically, 20 ml of 0.02 M prepared Zn $(Ac)_2$ solution and 0.1 ml of MPA solution were mixed with 80 ml water, and the pH of the solution was adjusted to 11.2 by dropwise addition of 1.0 M NaOH solution with stirring. The solution was placed in a four-necked flask in N_2 environment. Freshly prepared NaHSe solution was added through a syringe into the Zn-MPA precursor solution at room temperature under stirring. Then the mixture was heated to reflux (95°C) under atmospheric conditions with a condenser attached for 2 h to obtain ZnSe QDs.

Synthesis of $G_{16\text{-}6\text{-}16}$ protected ZnSe QDs: different concentrations of $G_{16\text{-}6\text{-}16}$ were added to the ZnSe QDs under vigorous stirring, and then these prepared $G_{16\text{-}6\text{-}16}$ protected ZnSe QDs solutions were ready for the following experiments.

3. Results and discussion: The obtained ZnSe QDs were characterised by HRTEM, X-ray powder diffraction spectrometry (XRD), UV-vis spectrometry and fluorescence spectrometry. The HRTEM images showed that ZnSe QDs were monodispersed and displayed an average diameter of about 5 nm (Fig. 1). Fig. 2 is the X-ray diffraction spectra of the prepared ZnSe QDs. The main diffraction peaks in the 2θ range of 20°–70° were corresponding to the (111), (220), (311) and (331) four lattice planes of the cubic sphalerite structure of ZnSe, which is consistent with JCPDS Card No. 37-1463. The diffraction peaks were obvious and had no other diffraction impurity peaks, which showed that the ZnSe QDs were well crystallised and were of high purity. As shown in Fig. 3, ZnSe QDs had a rather wide absorption band and its typical exciton absorption peak was at 350 nm, which is consistent with the reported MPA-capped ZnSe QDs [39]. The fluorescence excitation and emission wavelength of ZnSe QDs were 355 and 465 nm, respectively, (Fig. 4).

We investigated the influence of the molar ratio between ZnSe QDs (1 mM) and Gemini surfactant $G_{16\text{-}6\text{-}16}$ ($R_{\text{ZnSe QDs/G16-6-16}}$) on the fluorescence intensity of $G_{16\text{-}6\text{-}16}$ protected ZnSe QDs from 0 to 25:17. As shown in Figs. 5 and 6, the fluorescence intensity of the $G_{16\text{-}6\text{-}16}$ protected ZnSe QDs reduced at first, then increased quickly with increasing surfactant concentration and finally became stable. The surface tension of the QDs was decreased at first when $G_{16\text{-}6\text{-}16}$ was added, which resulted in the decrease of the fluorescence intensity. Then the surfactant $G_{16\text{-}6\text{-}16}$ formed a layer of hydrophilic film on the surface of the QDs

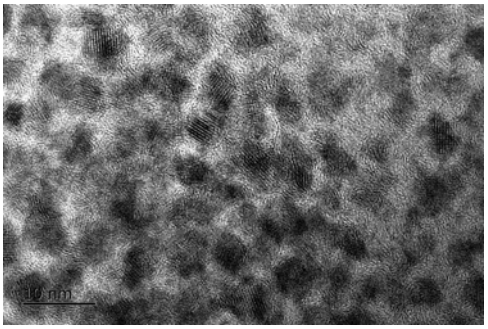

Figure 1 *HRTEM images of the as-prepared ZnSe QDs*

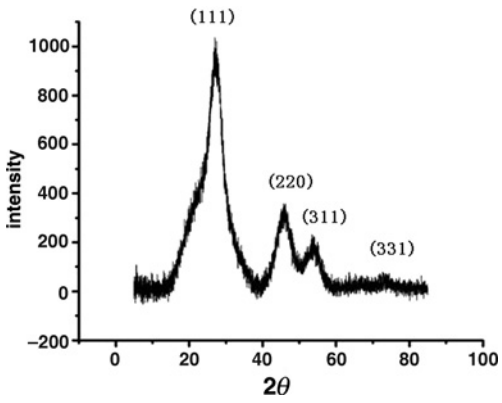

Figure 2 *XRD patterns of the as-prepared ZnSe QDs*

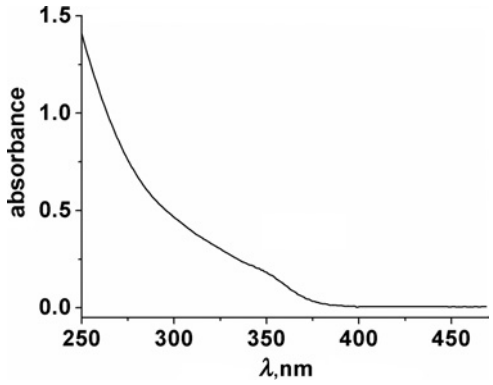

Figure 3 *Absorption spectra of the as-prepared ZnSe QDs*

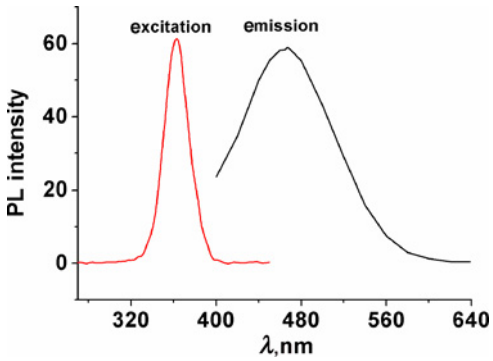

Figure 4 *Fluorescence spectra of the as-prepared ZnSe QDs*

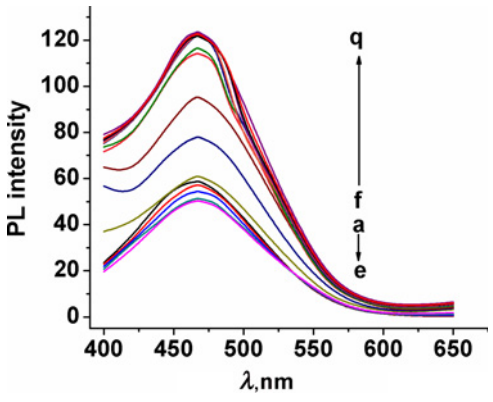

Figure 5 *Effect of the $R_{ZnSe\ QDs/G16\text{-}6\text{-}16}$ (a–e: 0–25:4; f–q: 25:6–25:17) on the fluorescence intensity of the $G_{16\text{-}6\text{-}16}$ protected ZnSe QDs nanomaterial*

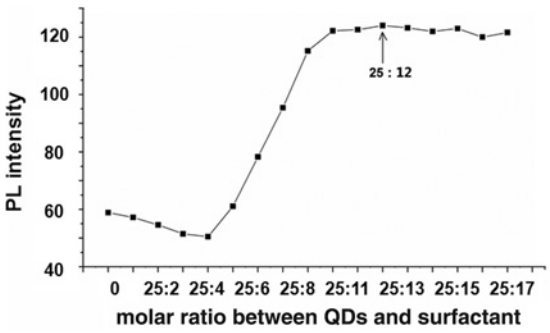

Figure 6 *Fluorescence signals of the $G_{16\text{-}6\text{-}16}$ protected ZnSe QDs nanomaterial synthesised with different $R_{ZnSe\ QDs/G16\text{-}6\text{-}16}$*

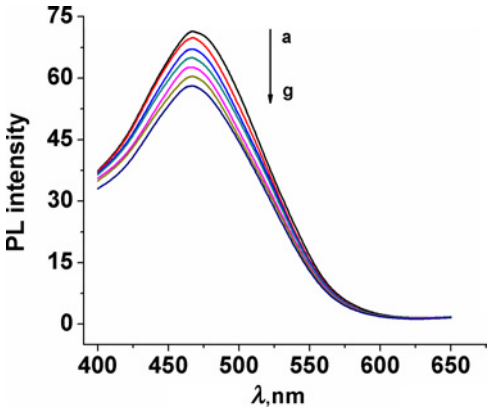

Figure 7 *Fluorescence spectra of $G_{16\text{-}6\text{-}16}$ protected ZnSe QDs nanomaterial in the presence of various concentrations of BSA (nM, a–g: 0.0, 10, 20, 30, 50, 60 and 80)*

with the increasing concentration of $G_{16\text{-}6\text{-}16}$, which can prevent the aggregation of QDs and increase the stability of QDs in aqueous media; thus, the fluorescence intensity increased. To obtain highly fluorescent $G_{16\text{-}6\text{-}16}$ protected ZnSe QDs nanomaterial, 25:12 was chosen as the optimal proportion in all experiments.

The reaction between $G_{16\text{-}6\text{-}16}$ protected ZnSe QDs and BSA at room temperature occurred rapidly. We can see from Fig. 7 that the fluorescence intensity of $G_{16\text{-}6\text{-}16}$ protected ZnSe QDs at 465 nm can be quenched by BSA and was linearly proportional to BSA (Fig. 8) over a concentration range from 0 to 80 nM with a correlation equation of $\Delta F = 0.52 + 16.9\ C$ (nM) and a correlation coefficient of 0.993. The detection limit (LOD) was 12.4 nM.

The fluorescence quenching is usually divided into static quenching and dynamic quenching. The dynamic quenching can be described by Stern–Volmer's equation (1), whereas the static quenching can be described by the Lineweaver–Burk equation (2) [40–41]

$$F_0/F = 1 + K_{SV}[Q] \tag{1}$$

$$1/(F_0 - F) = 1/F_0 + K_{LB}/F_0[Q]F_0/F = 1 + [Q]/K_{LB} \tag{2}$$

where F_0 and F are the steady-state fluorescence intensities in the absence and presence of quencher, respectively. $[Q]$ is the concentration of quencher, BSA. K_{SV} is the Stern–Volmer quenching constant and K_{LB} is the static quenching constant [42–45]. The relationship between $(F_0 - F)^{-1}$ and 1/[BSA] does not follow the Lineweaver–Burk equation. However, the linear relationship between F_0/F and the concentration of BSA showed that the fluorescence quenching followed the Stern–Volmer's equation; that is, dynamic quenching occurs (Fig. 9). The quenching rate K_{SV} can

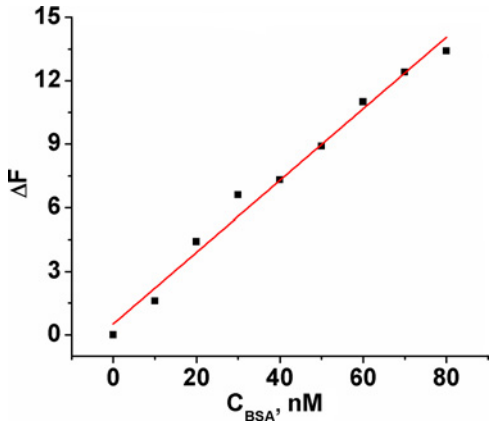

Figure 8 *Change of fluorescence signals of the $G_{16\text{-}6\text{-}16}$ protected ZnSe QDs nanomaterial at 460 nm against the concentration of BSA from 0 to 80 nM*

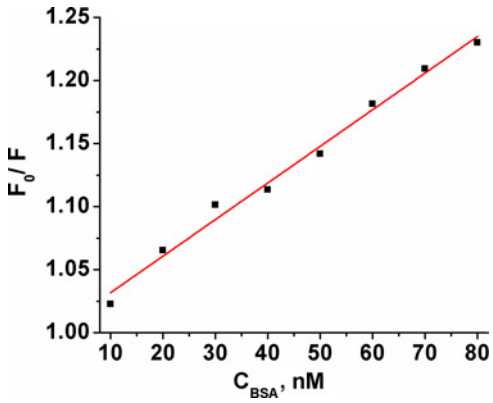

Figure 9 *Stern–Volmer's plot of fluorescence quenching of $G_{16\text{-}6\text{-}16}$ protected ZnSe QDs nanomaterial by BSA*

be obtained by linear Stern–Volmer plots of F_0/F against $[Q]$ from (1). As shown in Fig. 10 and Table 1, the K_{SV} of $G_{16\text{-}6\text{-}16}$ protected ZnSe QDs synthesised with $R_{ZnSe\ QDs/G16\text{-}6\text{-}16}$ of 25:12 was higher than that of 25:4, which further confirmed that 25:12 was the optimal proportion. We considered the hydrophobic effect between the $G_{16\text{-}6\text{-}16}$ on the surface of $G_{16\text{-}6\text{-}16}$ protected ZnSe QDs and BSA played a decisive effect in the fluorescence quenching of $G_{16\text{-}6\text{-}16}$ protected ZnSe QDs by BSA [38]. We also investigated the influence of BSA on the fluorescence intensity of ZnSe

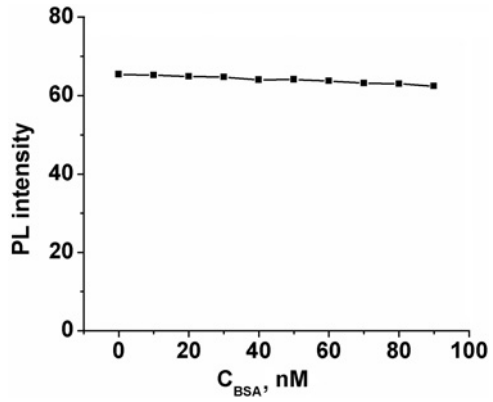

Figure 10 *Fluorescence signals of the ZnSe QDs in the presence of various concentrations of BSA (CZnSe QDs = 1 mM)*

doi: 10.1049/mnl.2014.0698

Table 1 Stern–Volmer quenching constants of BSA to $G_{16\text{-}6\text{-}16}$ protected ZnSe QDs nanomaterial synthesised with different $R_{ZnSe\ QDs/G16\text{-}6\text{-}16}$

$R_{ZnSe\ QDs/G16\text{-}6\text{-}16}$	K_{SV}	R
25:12	2.91×10^6	0.995
25:4	1.04×10^6	0.964

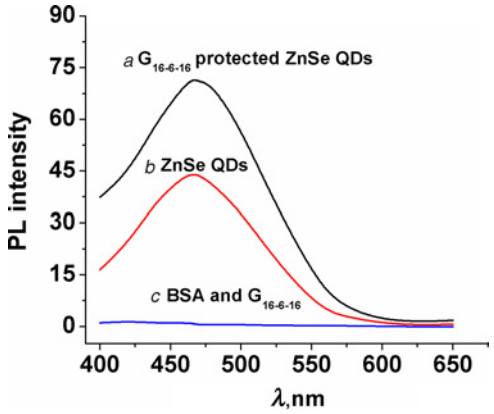

Figure 11 *Fluorescence spectra of a $G_{16\text{-}6\text{-}16}$ protected ZnSe QDs nanomaterial (a); ZnSe QDs (b); BSA and $G_{16\text{-}6\text{-}16}$ (c)*

QDs. Results have shown that BSA cannot quench the fluorescence intensity of ZnSe QDs (Fig. 11). The fluorescence intensity of $G_{16\text{-}6\text{-}16}$ protected ZnSe QDs was higher than the ZnSe QDs and the mixture of BSA and $G_{16\text{-}6\text{-}16}$ had no fluorescence signals at a wavelength range of 400–650 nm which facilitated our sensing approach (Fig. 12).

To evaluate the potential of the proposed $G_{16\text{-}6\text{-}16}$ protected ZnSe QDs-based fluorescent sensor for detecting proteins such as BSA, the interferences on the determination of BSA were studied, including relative acids and metal ions (Table 2). From the results, most interferents were unaffected by the change of fluorescence emission even at a rather high concentration. Although interferents such as RNA and DNA can affect the determination, diluting the samples with water can minimise the interference of coexisting substances in real samples. Thus, it is possible to use this method for the determination of proteins in real samples.

To demonstrate the applicability of the $G_{16\text{-}6\text{-}16}$ protected ZnSe QDs-based fluorescence probe, we detected the concentration of BSA in urine samples. The analytical results for the urine samples are shown in Table 3. The recoveries of spiked BSA ranged from 90 to 110%, which indicated no interference from urine samples. The relative standard deviation is lower than 5%,

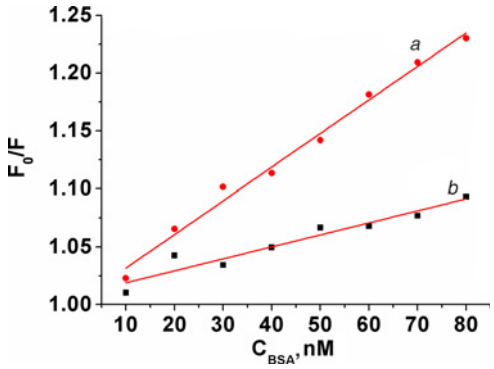

Figure 12 *Stern–Volmer's plot of fluorescence quenching of $G_{16\text{-}6\text{-}16}$ protected ZnSe QDs nanomaterial (C = 0.2 mM) synthesised with different RZnSe QDs/$G_{16\text{-}6\text{-}16}$ by BSA (RZnSe QDs/$G_{16\text{-}6\text{-}16}$, a = 25:12; and b = 25:4)*

Table 2 Effect of co-existing substances on the change of fluorescence emission because of the addition of BSA at 1.33 nM

Substance	Concentration, $ng \cdot l^{-1}$	Change of the fluorescence intensity, %
Mn^{2+}	330	2.4
Fe^{3+}	0.033	3.6
Ca^{2+}	133	4.5
Al^{3+}	0.2	−4.8
Mg^{2+}	28	2.6
K^{+}	68.9	2.5
Cu^{2+}	1	−4.2
Zn^{2+}	0.117	2.4
Na^{+}	46.7	0.1
RNA (Mw = 330)	0.0017	−2
DNA (Mw = 66 000)	0.00087	2.7
glucose	0.002	−1.9
L-histidine	0.017	1.9
L-glycine	0.283	−2.4
arginine	0.174	1.8
lysine	0.146	2.9
isoleucine	0.131	1.4
urea	0.06006	1.3
L-cysteine	0.121	2.4
L-tryptophan	0.204	2.7

Table 3 Determination of BSA in urine samples using the proposed method

Matrix	Urine		
BSA, nM	1.00	1.33	1.67
dilution ratio	200	200	200
recovery, %	110	110	90
regression equation		$Y = 0.52 + 16.9X$	
R		0.993	
LOD, nM		0.04	
RSD, %		4.9	

which also shows the good precision of this method. The above results demonstrate that the developed assay offers great potential for specific detection of proteins such as BSA in urine samples.

4. Conclusion: In this Letter, we used the Gemini surfactant hexamethylene-1,3-bis(cetyldimethylammonium bromide) ($G_{16\text{-}6\text{-}16}$) to modify ZnSe QDs and have successfully synthesised $G_{16\text{-}6\text{-}16}$ protected low-toxicity ZnSe QDs. As a high fluorescence efficiency nanomaterial that possesses excellent physical and chemical properties, $G_{16\text{-}6\text{-}16}$ protected ZnSe QDs have been introduced as a new fluorescent platform for sensing BSA. This method was simple, fast, selective and sensitive. Surfactant $G_{16\text{-}6\text{-}16}$ can interact with proteins through hydrophobic effect, thus leading to the fluorescence quenching of $G_{16\text{-}6\text{-}16}$ protected ZnSe QDs nanometre material, which facilitated our sensing approach. Furthermore, we validated the practicality of this method through an analysis of BSA in urine samples.

5. Acknowledgments: This work was financially supported by the Scientific Research Foundation of Education Commission of Hubei Province (Q20111010 and T201101), the Natural Science Foundation of Hubei Province (2011CDB059 and 2011CDA111), Research Fund for the Doctoral Program of Higher Education of China (20114208120006) and the National Undergraduate

Training Programs for Innovation and Entrepreneurship (201210512006 and 201210512020).

6 References

[1] Sriyam S., Sinchaikul S., Tantipaiboonwong P., Tzao C., Phutrakul S., Chen S.T.: 'Enhanced detectability in proteome studies', *J. Chromatogr. B*, 2007, **849**, pp. 91–104

[2] Anderson N.L., Polanski M., Pieper R., *ET AL.*: 'The human plasma proteome – a nonredundant list developed by combination of four separate sources', *Proteomics*, 2004, **3**, pp. 311–326

[3] Pieper R., Gatlin C.L., Makusky A.J., *ET AL.*: 'The human serum proteome: Display of nearly 3700 chromatographically separated protein spots on two-dimensional electrophoresis gels and identification of 325 distinct proteins', *Proteomics*, 2003, **3**, pp. 1345–1364

[4] Wulfkuhle J.D., Liotta L.A., Petricoin E.F.: 'Proteomic applications for the early detection of cancer', *Nat. Rev. Cancer*, 2003, **3**, pp. 267–275

[5] Zhang H.J., Lu Y.H., Long Y.J., *ET AL.*: 'An aptamer-functionalized gold nanoparticle biosensor for the detection of prion protein', *Anal. Methods*, 2014, **6**, pp. 2982–2987

[6] Li Y.K.: 'Quantitative detection of proteins by [Co (NH3)6]3+-DNA probe of resonance light scattering technique', *Asian J. Chem.*, 2013, **25**, pp. 8769–8771

[7] Xue Z.J., Zhang X.J., Wang G., Zhang D., Zhou H.C.: 'Determination of human serum albumin with tetra-amino copper phthalocyanine by resonance light scattering technique', *Asian J. Chem.*, 2013, **25**, pp. 529–532

[8] Baj S., Krawczyk T., Pradel N., *ET AL.*: 'Carbon nanofiber-based luminol-biotin probe for sensitive chemiluminescence detection of protein', *Anal. Sci.*, 2014, **30**, pp. 1051–1056

[9] Zor T., Selinger Z.: 'Linearization of the Bradford protein assay increases its sensitivity: theoretical and experimental studies', *Anal. Biochem.*, 1996, **236**, pp. 302–308

[10] Xu S.H., Liu P.P., Lu X., *ET AL.*: 'A highly sensitive 'turn-on' fluorescent sensor for the detection of human serum proteins based on the size exclusion of the polyacrylamide gel', *Electrophoresis*, 2014, **35**, pp. 546–553

[11] Jaiswal P., Jha S.N., Borah A., Gautam A., Grewal M.K., Jindal G.: 'Detection and quantification of soymilk in cow-buffalo milk using attenuated total reflectance Fourier transform infraredspectroscopy (ATR-FTIR)', *Food Chem.*, 2014, **168**, pp. 41–47

[12] Briere L.K., Brandt J.M., Medley J.B.: 'Measurement of protein denaturation in human synovial fluid and its analogs using differential scanning calorimetry', *J. Therm. Anal. Calorim.*, 2010, **102**, pp. 99–106

[13] Michalet X., Pinaud F.F., Bentolila L.A., *ET AL.*: 'Quantum dots for live cells, in vivo imaging, and diagnostics', *Science*, 2005, **307**, pp. 538–544

[14] Murphy C.J.: 'Optical sensing with quantum dots', *Anal. Chem.*, 2002, **74**, pp. 520 A–526 A

[15] Reiss P., Quemarda G., Carayon S., Bleuse J., Chandezon F., Pron A.: 'Luminescent ZnSe nanocrystals of high color purity', *Mater. Chem. Phys.*, 2004, **84**, pp. 10–13

[16] Jamieson T., Bakhshi R., Petrova D., Pocock R., Imani M., Seifalian A.M.: 'Biological applications of quantum dots', *Biomaterials*, 2007, **28**, pp. 4717–4732

[17] Balti I., Chevallie P., Menager C., *ET AL.*: 'Nanocrystals of Zn(Fe)O-based diluted magnetic semi-conductor as potential luminescent and magnetic bimodal bioimaging probes', *RSC Adv.*, 2014, **4**, pp. 58145–58150

[18] Kolny-Olesiak J., Weller H.: 'Synthesis and application of colloidal $CuInS_2$ semiconductor nanocrystals', *ACS Appl. Mater. Interfaces*, 2013, **5**, pp. 12221–12237

[19] Pisanic T.R., Zhang Y., Wang T.H.: 'Quantum dots in diagnostics and detection: principles and paradigms', *Analyst*, 2014, **139**, pp. 2968–2981

[20] Knudsen B.R., Jepsen M.L., Ho Y.P.: 'Quantum dot-based nanosensors for diagnosis via enzyme activity measurement', *Expert Rev. Mol. Diagn.*, 2013, **13**, pp. 367–375

[21] Derfus A.M., Bhatia S.N.: 'Probing the cytotoxicity of semiconductor quantum dots', *Nano Lett.*, 2004, **4**, pp. 1l–18

[22] Fu T., Qin H.Y., Hu H.J., Hong Z., He S.L.: 'Aqueous synthesis and fluorescence-imaging application of CdTe/ZnSe core/shell quantum dots with high stability and low cytotoxicity', *J. Nanosci. Nanotechnol.*, 2010, **10**, pp. 1741–1746

[23] Ding Y.L., Shen S.Z., Sun H.D., Sun K.N., Liu F.T.: 'Synthesis of L-glutathione-capped-ZnSe quantum dots for the sensitive and selective determination of copper ion in aqueous solutions', *Sens. Actuators B*, 2014, **203**, pp. 35–43

[24] Shi B.Q., Cai Z.X., Ma M.H.: 'A facile colloid aqueous method for synthesis of water soluble ZnSe quantum dots with high fluorescence and stability characterization', *Spectrosc. Spectral Anal.*, 2010, **3**, pp. 720–724

[25] Li L., Zhang F.F., Ding Y.P., Wang Y.P., Zhang L.L.: 'Synthesis of functionalized ZnSe nanoparticles and their applications in the determination of bovine serum albumin', *J. Fluoresc.*, 2009, **19**, pp. 437–441

[26] Reiss P.: 'ZnSe based colloidal nanocrystals: synthesis, shape control, core/shell, alloy and doped systems', *New J. Chem.*, 2007, **31**, pp. 1843–1852

[27] Tardioli S., Bonincontro A., Mesa C.L., Muzzalupo R.: 'Interaction of bovine serum albumin with Gemini surfactants', *J. Colloid Interface Sci.*, 2010, **347**, pp. 96–101

[28] Chen Z.G., Liu G.L., Chen M.H., Peng Y.R., Wu M.Y.: 'Determination of nanograms of proteins based on decreased resonance light scattering of zwitterionic Gemini surfactant', *Anal. Biochem.*, 2009, **384**, pp. 337–342

[29] Zou Q.C., Chen H., Yu H., Zhang J.Z., Chai S.G., Wu L.M.: 'Synthesis of polycation with Gemini structure and detection of DNA by resonance light scattering', *Sens. Actuators B*, 2010, **145**, pp. 378–385

[30] Zhao X.F., Shang Y.Z., Hu J., Liu H.L., Hu Y.: 'Biophysical characterization of complexation of DNA with oppositely charged Gemini surfactant 12–3–12', *Biophys. Chem.*, 2008, **138**, pp. 144–149

[31] Gull N., Sen P., Khan R.H., Kabir-ud-Din.: 'Interaction of bovine (BSA), rabbit (RSA), and porcine (PSA) serum albumins with cationic single-chain/Gemini surfactants: a comparative study', *Langmuir*, 2009, **25**, pp. 11686–11691

[32] Bai H.Y., Qian J.H., Tian H.Y., Pan W.W., Zhang L.Y., Zhang W.B.: 'Fluorescent polarity probes for identifying bovine serum albumin: Amplification effect of para-substituted benzene', *Dyes Pigm.*, 2014, **103**, pp. 1–8

[33] Mandeville J.S., Tajmir-Riahi H.A.: 'Complexes of dendrimers with bovine serum albumin', *Biomacromolecules*, 2010, **11**, pp. 465–472

[34] Xiong X., Song F., Sun S., Fan J., Peng X.: 'Red-emissive fluorescein derivatives and detection of bovine serum albumin', *Asian J. Org. Chem.*, 2013, **2**, pp. 145–149

[35] Zhang K., Song C., Li Q., Li Y., Sun Y., Yang K.: 'The establishment of a highly sensitive ELISA for detecting bovine serum albumin (BSA) based on a specific pair of monoclonal antibodies (mAb) and its application in vaccine quality control', *Hum. Vaccin.*, 2010, **6**, pp. 652–658

[36] Qian J., Xu Y., Qian X.: 'Logically sensing aggregate process and discriminating SDS from other surfactants with the assistance of BSA', *Chin. J. Chem.*, 2012, **30**, pp. 1283–1288

[37] Chodankar S., Aswal V.K., Hassan P.A., Wagh A.G.: 'Structure of protein surfactant complexes as studied by small-angle neutron scattering and dynamic light scattering', *Phys. B, Phys. Condensed Matter.*, 2007, **398**, pp. 112–117

[38] Lehres S.: 'Solute perturbation of protein fluorescence: the quenching of the tryptophyl fluorescence of model compounds and of lysozyme by iodide ion', *Biochemistry.*, 1971, **10**, pp. 3254–3258

[39] Ruan X.J., Wang B.B., Ma M.H., Guo A.Z., Cai Z.X.: 'Application of water-soluble ZnSe quantum dots on rapid and sensitive detection of MPB83 protein on surface of *Mycobacterium bovis*', *Chin. J. Anal. Chem.*, 2014, **42**, pp. 643–647

[40] Sauer K., Scheer H., Sauer P.: 'Förster transfer calculations based on crystal structure data from *Agmenellum quadruplicatum* C-Phycocyanin', *Photochem. Photobiol.*, 1987, **46**, pp. 427–440

[41] Lakowicz J.R., Weber G.: 'Quenching of protein fluorescence by oxygen. Detection of structural fluctuations in proteins on the nanosecond time scale', *Biochemistry*, 1973, **12**, pp. 4171–4179

[42] Jones R.M., Bergstedt T.S., McBranch D.W., Whitten D.G.: 'Tuning of superquenching in layered and mixed fluorescent polyelectrolytes', *J. Am. Chem. Soc.*, 2001, **123**, pp. 6726–6727

[43] Murphy C.B., Zhang Y., Troxler T., Ferry V., Martin J.J., Jones W.E.: 'Probing Förster and Dexter energy-transfer mechanisms in fluorescent conjugated polymer chemosensors', *J. Phys. Chem. B*, 2004, **108**, pp. 1537–1543

[44] Baptista M.S., Indig G.L.: 'Effect of BSA binding on photophysical and photochemical properties of triarylmethane dyes', *J. Phys. Chem. B*, 1998, **102**, pp. 4678–4688

[45] Lakowicz J.R.: 'Principle of fluorescence spectroscopy' (Plenum Press, New York, 1999, 2nd edn.)

doi: 10.1049/mnl.2014.0698